Structure Determination of Gas-Phase Niobium and Tantalum Carbide Nanocrystals via Infrared Spectroscopy

Deniz van Heijnsbergen,[1,2] André Fielicke,[1] Gerard Meijer,[1,2] and Gert von Helden[1]

[1]FOM Institute for Plasma Physics Rijnhuizen, Edisonbaan 14, NL-3439 MN Nieuwegein, The Netherlands
[2]Department of Molecular and Laser Physics, University of Nijmegen, Toernooiveld 1, NL-6525 ED Nijmegen, The Netherlands

Niobium and tantalum carbide clusters have been isolated in the gas phase and irradiated with intense tunable infrared (IR) light. Stable neutral clusters are selectively ionized and subsequently detected in a mass spectrometer. By tuning the IR frequency, infrared multiphoton absorption spectra are obtained for a whole range of clusters. These mass-selective IR spectra lead to insights into the structures of small niobium and tantalum carbide clusters and nanocrystals.

Gas-phase metal carbide clusters appear in a variety of stoichiometries and with different structures. Most of the knowledge on their structures and building principles has been obtained from the analysis of mass spectral abundance patterns. Proposed structures range from the cage-like met-car structure for the unique M_8C_{12} stoichiometry to cubic lattice structures, which are suggested to be similar to the bulk structures of carbides [1–5]. To get more direct information on the structure of metal carbide clusters, different experimental methods have been applied, such as photofragmentation [3,6], photoionization in combination with quantum chemical calculations [7–9], or gas-phase ion chromatography [10,11]. Reactions with chlorine, oxygen, carbon monoxide, and various organic molecules can be used to probe the coordination of the "surface" atoms of the clusters [12–14]. Recently, we reported the application of the infrared resonance enhanced multiphoton ionization (IR-REMPI) technique to obtain vibrational spectra of the titanium met-car Ti_8C_{12} [15] as well as of small titanium and vanadium carbide nanocrystals starting with the $M_{14}C_{13}$ stoichiometry [16,17].

For niobium carbide clusters, it has been shown previously that the relative abundance of the different cluster types, either met-car or nanocrystalline structures, is very sensitive to the formation conditions [3,18]. In comparison, for the carbide clusters of the heavier homologue of niobium, tantalum, it has been suggested that the cubic structures are preferred [4]. Recently, small tantalum carbide clusters up to Ta_6C_7 have been investigated by Heaven *et al.* [9] using multiphoton ionization. On the basis of accompanying density functional theory (DFT) calculations for Ta_4C_4, a distorted cubic shape with C_{2v} symmetry is proposed [9], while for Nb_4C_4 a nearly perfect cube with T_d symmetry is predicted by Harris *et al.* [19]. In contrast to these calculations, the reaction of Nb_4C_4 with O_2 results in loss of two carbon atoms, which led to the proposal of a cubic structure containing Nb_2 and C_2 units instead of an alternating Nb and C atoms order [13].

In this study, we focus on the experimental determination of the building principles of gas-phase niobium and tantalum carbide clusters using infrared spectroscopy. For this, gas-phase niobium and tantalum carbide clusters are produced with a standard laser ablation source using 5% methane in He as a carrier gas. The experimental details have been described previously [15]. The neutral clusters in the molecular beam are irradiated with the focused infrared light produced by FELIX [20], the "Free Electron Laser for Infrared eXperiments." When the laser is on resonance with a vibrational transition, the clusters rapidly absorb multiple IR photons, making them quite hot. These hot clusters have now several possible cooling pathways. Clusters for which the ionization potential (IP) is low compared to the dissociation energy will undergo thermionic emission of electrons, acquiring positive charges. Clusters with lower dissociation energies relative to their IP's will tend to fragment, but will not necessarily form ions. The ions produced are subsequently detected with a standard reflectron time-of-flight mass spectrometer. Measuring the intensity of a certain cluster ion as a function of IR wavelength results in the infrared multiple photon absorption spectrum of the neutral cluster. The internal energy distribution of the clusters before IR irradiation is not known, but from the source conditions we estimate the cluster temperature to be in the range between 300–1500 K.

The mass spectrum in Fig. 1 shows the niobium carbide cluster ion distribution that has been obtained by IR multiphoton ionization. For this, 120 individual mass spectra out of the 400−770 cm^{-1} range have been integrated. Surprisingly, a whole series of specific masses is observed, and the stoichiometry of the corresponding ions can be unambiguously identified. The prominent peaks in this mass spectrum are accompanied by a set of two numbers, indicating the number of niobium and carbon atoms, respectively. Throughout this paper we use the notation (x, y) to indicate the cluster M_xC_y. Mass peaks are observed to occur in groups with the most intense peak in each group occurring near a metal to carbon ratio of 1. Within such a group, peaks are spaced by 12 mass units corresponding to one carbon atom. The cluster with the highest intensity is $Nb_{14}C_{13}$. Prominent cluster peaks with such a stoichiometry have been observed previously for niobium and other metals. There is strong evidence that the (14, 13) cluster
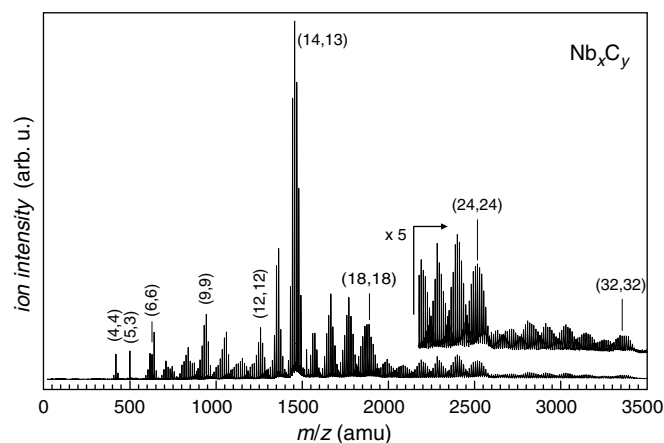
FIG. 1. Thermionic emission mass spectrum of niobium carbide clusters after excitation with infrared light. Averaged spectrum over the 400−770 cm^{-1} region.

belongs to a family of nanocrystals where the metal and carbon atoms are arranged in a similar fashion as in the face centered cubic (fcc) lattice of bulk NbC. $Nb_{14}C_{13}$ is the 3 atoms by 3 atoms by 3 atoms ($3 \times 3 \times 3$) member in the family. For clusters larger than (14, 13), the observed mass peaks can be explained by fcc crystallite structures as well. The overall intensity pattern in the mass spectra shows the series after which the relative intensity drops. These drops occur approximately after signals corresponding to (18, 18), (24, 24), and (32, 32) clusters coinciding with geometrical shell closings of $3 \times 3 \times 4$, $3 \times 4 \times 4$, and $4 \times 4 \times 4$ cuboids, respectively. Further cluster intensity drops are observed behind (40, 40) and (50, 50), which correspond to $4 \times 4 \times 5$ and $4 \times 5 \times 5$ nanocrystals.

The high signal intensity of the (14, 13) cluster can be caused by several different aspects. Besides the abundance in the molecular beam, the efficiency of the IR multiphoton absorption process as well as of the ionization process are important. The efficiency of the multiphoton absorption process is determined by the anharmonicity of the mode, the bandwidth, and the wavelength of FELIX. The ionization process is influenced by the value of the IP relative to the cluster's fragmentation energy. According to recent calculations carried out by Harris et al. [19], $Nb_{14}C_{13}$ has a rather low ionization potential of 3.9 eV, while the binding energy per atom (D_0) exceeds 6 eV.

For titanium and vanadium, the smallest nanocrystalline cluster observed using IR-REMPI is (14, 13). Surprisingly, peaks corresponding to masses lower than that of (14, 13) are observed in the case of niobium carbide. The lowest peak observed corresponds to Nb_4C_4. Looking at ions that are emitted from a cluster source, $Nb_4C_4^+$ has been identified previously and is suggested to be the smallest ($2 \times 2 \times 2$) cubic crystal [3]. Exchanging one carbon atom for a niobium atom results in Nb_5C_3.

By tuning FELIX's wavelength while monitoring the mass selected ion yield, the infrared spectra of the clusters can be obtained. In the present experiment, FELIX is

tuned from 370 to 1650 cm^{-1}, and the infrared spectra of all stable clusters shown in Fig. 1 are measured simultaneously. In Fig. 2 the infrared spectra of selected masses are shown. Above 760 cm^{-1}, the ion yield is low and shows no clear wavelength dependence. A single broad resonance is observed for the smallest two clusters, (4, 4) and (5, 3) with the maxima at 675 and 660 cm^{-1}, respectively. This resonance narrows significantly when going to (6, 6) and (9, 9) and shifts to 680 cm^{-1} for (9, 9). Following the evolution of this peak to larger clusters, a gradual shift to 630 cm^{-1} is observed, and the intensity of this peak decreases with increasing cluster size. A new peak is observed for the (9, 9) cluster at 520 cm^{-1}. This peak is very weak for the (9, 9) cluster but becomes dominant at about (14, 13). Its position shifts continuously from 505 cm^{-1} for (14, 13) to 480 cm^{-1} for (50, 50). The infrared spectra of $Nb_{14}C_{13}$ and the larger clusters are very similar. The two modes are observed for up to at least (32, 32). However, the mode around 650 cm^{-1} becomes very low in relative intensity.

The mass distribution of ionized tantalum carbide clusters, obtained by IR multiphoton ionization averaged over
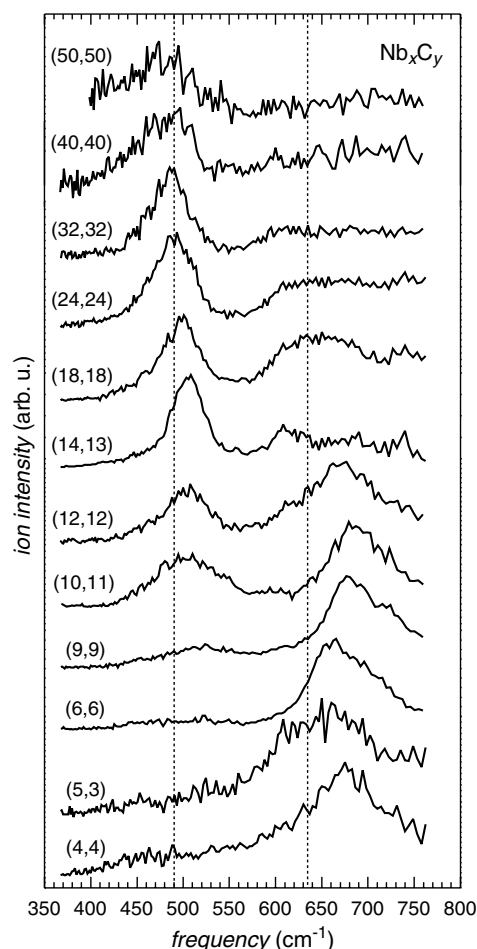

FIG. 2. Infrared spectra for several Nb_xC_y clusters, indicated as (x, y). Except the (5, 3) all clusters may be viewed as parts of a fcc lattice. The two dashed lines indicate the frequencies of optical active surface vibrational modes of fcc NbC (100) measured by EELS [21].

the 400–770 cm^{-1} range, is shown in Fig. 3. The cluster distribution is similar to the one observed for niobium carbide with the maximum corresponding to the $(4,4)$ cluster and intensity drops behind the signals assigned to the $(14,13)$, $(18,18)$, and $(24,24)$ clusters, which are again consistent with geometrical shell closings of cubic nanocrystals. Infrared spectra of tantalum carbide clusters are presented in Fig. 4. The spectra exhibit two absorption bands, one that shifts slightly from 505 cm^{-1} towards 480 cm^{-1} with increasing cluster size and the second around 670 cm^{-1}. Apart from the exact peak positions, the spectra appear to be similar to the corresponding niobium carbides: The 670 cm^{-1} absorption is dominant for the clusters up to $(9,9)$ when the second band at 505 cm^{-1} begins to grow in. For larger clusters [up to $(24,24)$] both bands exhibit comparable intensities.

The experimental spectra of the clusters presented here can be compared to theory as well as to data available for the bulk phase. Recently, vibrational spectra of small niobium carbide clusters have been calculated by Harris and Dance [19]. For the Nb_4C_4 cluster, a cubic ground state is found, and intense IR active modes are predicted at 671, 588–611, 440, and below 280 cm^{-1}. In comparison, the experimental spectrum in Fig. 2 shows only one broad band centered at 675 cm^{-1}. For the Nb_6C_6 cluster, bands are predicted at 702, 607–631, and 487 cm^{-1}. Also for this cluster, the experiment shows only one (broad) band around 665 cm^{-1}. The vibrational frequencies of Ta_4C_4 have been calculated as well and more than 10 modes have been found in the 300–800 cm^{-1} region [9]. Unfortunately, the relative intensities of the modes are not reported, which makes a direct comparison to the experimental data difficult.

Since IR-REMPI relies on multiple photon absorption, the ion yield depends on cluster parameters, such as vibrational anharmonicity and internal vibrational redistribution rates [22]. This may be one reason for the disagreement between experimental infrared spectra and theory. Another possible explanation is that the small
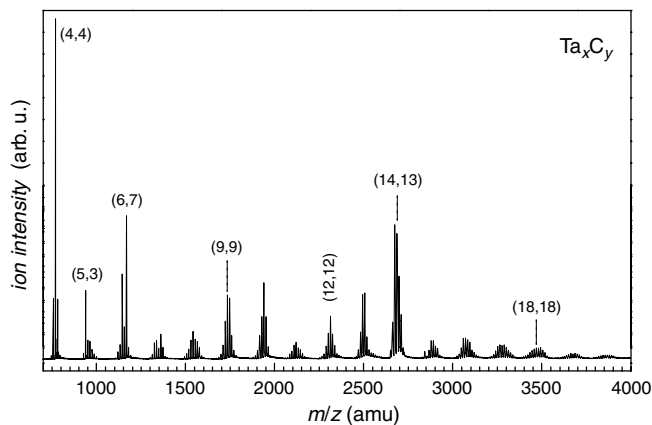
clusters in our experiment have a different structure than predicted on the basis of the DFT calculations. An alternative Nb_4C_4 isomer has been suggested by Deng *et al.* [13], in which C_2 units are present. From the infrared spectra shown here, there is no evidence for the presence of such an isomer. If it contains C═C units as in the met-cars, a strong signal would be expected in the C═C stretch region. For met-cars, this vibration corresponds to intense absorption in the 1200–1400 cm^{-1} range, e.g., for Ti_8C_{12} at 1395 cm^{-1} [15]. Since none of the presented clusters shows IR active modes higher than 800 cm^{-1}, that contradicts the proposed existence of C_2 units in the cluster structures, but supports the presence of isolated C atoms.

Both niobium as well as tantalum carbide are metallic in the solid. Their IR spectral properties are thus difficult to determine. However, electron energy loss spectroscopy (EELS) gives information on optically active (surface) phonon modes of these materials. In Fig. 2 we show also the positions of the EELS bands of the (100) surface of fcc NbC [21]. Two IR active bands have been identified, centered at 490 and 635 cm^{-1}. For fcc TaC (see Fig. 4), the position of the EELS peaks for the (100) surface are slightly shifted in comparison to NbC to 465 and 660 cm^{-1}, respectively [21].

Considering the enormous difference in dimensions and phase, the agreement between the gas-phase spectra of small niobium and tantalum carbide nanocrystals and the EELS spectrum of the bulk material with the fcc structure is striking. Although the infrared modes observed
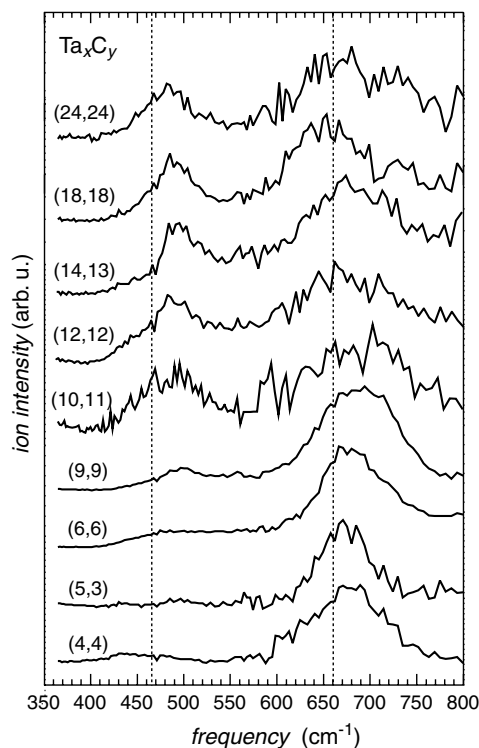

FIG. 3. Mass distribution of Ta_xC_{+y} cluster ions formed via thermionic emission. The mass spectrum has been integrated while FELIX is tuned through the 400–770 cm^{-1} region.

FIG. 4. Infrared multiphoton absorption spectra of selected Ta_xC_y clusters. The frequencies of optical active EELS bands of the TaC (100) surface are marked by the dashed lines [21].

experimentally are undoubtedly envelopes of a set of modes, detailed analysis of the data can unravel some basic properties about the nature of these modes.

Characteristic surface-localized optical modes of rock-salt structured crystals were found previously by Wallis *et al.* [23] and by Lucas [24] for NaCl (100). The "Wallis" mode is associated with out-of-plane vibrations (i.e., perpendicular to the surface), and the "Lucas" mode with in-plane vibrations (i.e., parallel to the surface). Similarly, Oshima *et al.* [21] assigned the modes in their EELS spectra as the motion of the light carbon atom parallel (higher frequency) or perpendicular (lower frequency) to the surface. Obviously, it is difficult to transfer such concepts to small clusters, where most atoms are located on corner or edge positions. Nonetheless, it is striking to see how the low frequency mode is negligible or not present at all for small clusters, but starts growing for the $(9, 9)$ cluster and becomes the dominant mode for clusters larger than $(14, 13)$. This trend is accompanied by an increasing mean coordination number of the carbon (and the metal) atoms.

The sudden growth of the low frequency band at about 500 cm^{-1} is connected with the transition from a two-layered to a three-layered structure between the $2 \times 3 \times 3$ $(9, 9)$ and the $3 \times 3 \times 3$ $(14, 13)$ clusters. This structure-related change of the IR spectrum allows one to analyze the geometry of intermediate clusters. For example, since the spectrum of the $(12, 12)$ cluster resembles the spectrum of the $(14, 13)$ rather than that of the $(9, 9)$ cluster, it is most likely that its structure is not the $2 \times 3 \times 4$ cuboid but a defective $(14, 13)$ cube, missing one carbon and two metal atoms (possibly one row on an edge of the cube). In general, both components, the metal and the carbon atoms, prefer a filled coordination sphere. Therefore, the defective cube structure should be preferred, because of the higher mean coordination number in comparison to the flat $2 \times 3 \times 4$ cluster. Based on the $(14, 13)$ cube, its defect structures may also contain a central carbon atom coordinated by six metal atoms. Possibly, the appearance of the 500 cm^{-1} band is connected to this structural element. In an analogous way, the spectral properties of the $(10, 11)$ cluster suggest its existence in the form of a $3 \times 3 \times 3$ cube with two missing edge rows. In these cases, the IR spectra directly indicate which types of isomers are preferred in the growth mechanism of metal carbide nanocrystals.

The results shown here demonstrate the potential that infrared spectroscopy of gas-phase clusters has when combined with mass selectivity. The patterns observed in the thermionic emission mass spectra of niobium and tantalum carbide clusters indicate geometric shell closings of cubic nanocrystals. Consistent with this, large clusters show IR spectra in which the optical surface phonons of the bulk can be clearly recognized. A clear break can be observed around $M_{10}C_{11}$, as smaller clusters have pronouncedly different IR spectra. These differences might be attribut-

able to a transition from a two-layered $(2 \times 3 \times 3)$ to a three-layered $(3 \times 3 \times 3)$ cluster structure. More elaborate theoretical calculations are needed to clarify this. The recent structural identification of Ti_8C_{12} [25] showed that experimental IR spectra of gas-phase clusters are a fruitful basis for such calculations.

[1] B. C. Guo, K. P. Kerns, and A. W. Castleman, Jr., Science **255**, 1411 (1992).
[2] J. S. Pilgrim and M. A. Duncan, J. Am. Chem. Soc. **115**, 9724 (1993).
[3] J. S. Pilgrim, L. R. Brock, and M. A. Duncan, J. Phys. Chem. **99**, 544 (1995).
[4] S. Wei *et al.,* Science **256**, 818 (1992).
[5] N. Blessing, S. Burkart, and G. Ganteför, Eur. Phys. J. D **17**, 37 (2001).
[6] J. Purnell, S. Wei, and A. W. Castleman, Jr., Chem. Phys. Lett. **229**, 105 (1994).
[7] L. R. Brock and M. A. Duncan, J. Phys. Chem. **100**, 5654 (1996).
[8] D.-S. Yang *et al.,* J. Chem. Phys. **105**, 10 663 (1996).
[9] M. W. Heaven *et al.,* J. Phys. Chem. A **104**, 3308 (2000).
[10] G. von Helden *et al.,* Chem. Phys. Lett. **227**, 601 (1994).
[11] S. Lee *et al.,* Science **267**, 999 (1995).
[12] C. S. Yeh *et al.,* J. Am. Chem. Soc. **117**, 4042 (1995); Y. G. Byun *et al.,* J. Phys. Chem. **100**, 6336 (1996); Y. G. Byun *et al.,* J. Phys. Chem. **100**, 14 281 (1996).
[13] H. T. Deng *et al.,* Int. J. Mass Spectrom. Ion Process. **167/168**, 615 (1997).
[14] H. T. Deng, K. P. Kerns, and A. W. Castleman, Jr., J. Am. Chem. Soc. **118**, 446 (1998).
[15] D. van Heijnsbergen *et al.,* Phys. Rev. Lett. **83**, 4983 (1999).
[16] G. von Helden *et al.,* Science **288**, 313 (2000).
[17] G. von Helden *et al.,* Chem. Phys. Lett. **333**, 350 (2001).
[18] S. Wei *et al.,* J. Am. Chem. Soc. **116**, 4475 (1994).
[19] H. Harris and I. Dance, J. Phys. Chem. A **105**, 3340 (2001).
[20] D. Oepts, A. F. G. van der Meer, and P. W. van Amersfoort, Infrared Phys. Technol. **36**, 297 (1995).
[21] C. Oshima *et al.,* Phys. Rev. Lett. **56**, 240 (1986); Solid State Commun. **57**, 283 (1986).
[22] G. von Helden *et al.,* Opt. Ex. **4**, 46 (1999).
[23] R. F. Wallis, D. L. Mills, and A. A. Maradudin, in *Localized Excitation in Solids,* edited by R. F. Wallis (Plenum, New York, 1968), p. 403.
[24] A. A. Lucas, J. Chem. Phys. **48**, 3156 (1968).
[25] G. K. Gueorguiev and J. M. Pacheco, Phys. Rev. Lett. **88**, 115504 (2002).